Arboriculture & Urban Forestry 2023
https://doi.org/10.48044/jauf.2023.030

Tree View Assessment: Survey of Two Municipalities Located in the Brussels Capital Region

By M. Llaguno-Munitxa, E. Agudo-Sierra, A. Burgueño-Diaz, and Alain Guillet

Abstract. Background: Recent literature has highlighted the importance of visual accessibility to nature to reduce stress, anxiety, or depression amongst others. However, green visual accessibility is yet rarely considered in urban policy implementations. Reasons behind this are manifold, and include the challenges associated with the measurability of green views which require data-intensive pedestrian view computations, and assessment methods are yet to be agreed upon. Methods: Two methods, Street View Images (SVI) and semantic classification, and geospatial viewshed analysis, were used to compute street level tree views. All street views contained within 2 municipalities from the Brussels Capital Region (BCR) have been studied. Using the SVI method, 15 green view indicators have been proposed. Using the viewshed analysis, the tree view area ratio (TV_{ar}) from each SVI geo-location has been computed. The independence between the indicators was evaluated, and using a random forest model, the principal SVI indicators to describe the TV_{ar} have been studied. Results: The variability explained by the random forest model was approximately 60% to 70%. The SVI indicators related to the horizontality of green infrastructure and tree canopy explained most of TV_{ar}. The results also reveal the tree canopy differences between both municipalities. Conclusions: SVI tree view indicators provide acceptable predictions of the TV_{ar} which could be particularly useful for municipalities with no access to detailed geospatial data. The 30% to 40% of the unexplained variability, could be related to errors derived from the tree canopy geospatial layer, differences in the data collection dates, or geolocation errors of the SVIs.

Keywords. Green Accessibility; Green Visibility; Tree Canopy; Tree Visibility; Viewshed Analysis.

INTRODUCTION

The benefits of urban green infrastructure accessibility for citizens' physical and mental health has been widely reported in prior literature (Hartig 2008; Hartig and Kahn 2016). The role visual accessibility to green infrastructure can play for urban stress, anxiety, or depression mitigation amongst others has been acknowledged (Huang et al. 2021; Konijnendijk 2023). However, while physical accessibility to green areas is starting to be assessed for urban policy implementations (van den Bosch and Ode Sang 2017), visual accessibility is yet rarely considered. In recent years, strategic tree planting investments have been allocated to enhance the tree accessibility in several cities. For example, the city of Liege, Belgium, put forward a 10-year tree planting plan named *Plan Canopee*, with the ambition to reach 24,000 trees planted (Ville de Liege 2007). Similarly, between 2007 and 2017, the Million Trees initiative in New York City successfully planted one million trees by promoting citizens' engagement to enhance the urban forest and reduce tree access inequality (Million Trees NYC 2017). Likewise, in Paris, a plan to plant 170,000 trees by 2026 was recently set (Masterson 2022). In 2018, the city of Frederiksberg, Denmark, introduced an ambitious policy that declared all inhabitants should be able to view at least one tree from their household, which builds on physical and visual tree accessibility principles (Frederiksberg Kommune 2018). However, urban tree planting strategies to account for tree view accessibility are still very limited. New approaches have been formulated, namely the 3-30-300 rule for urban forestry planning, which recommends a minimum of 3 trees visible from each building, no less than 30% tree canopy in every neighborhood, and a maximum distance of 300 m to the nearest green public space from every household (Konijnendijk 2023). However, measuring green views requires extensive participant surveys or data-intensive computations for which the assessment methods are yet to be agreed upon (Hu et al. 2023; Tabatabaie et al. 2023).

Tree view accessibility assessments utilizing participant questionnaires and surveys have proved to be very time consuming and resource intensive (de Vries et al. 2013; Triebner et al. 2019). On the other hand, given the increasing availability of Street View Imagery (SVI), various publications have made use of street level panoramic and fisheye photos to compute metrics such as the Green View Index (GVI) or Green Area Index (GAI) amongst others (Li et al. 2015; Ye et al. 2019). The possibilities to develop tools and strategies for geospatial tree viewshed computations are also starting to be discussed (Cimburova and Blumentrath 2022). Prior literature has also reported inconsistent results when comparing SVI and geospatial methods. For example, Urban Green Infrastructure (UGI) quantification results obtained through aerial imagery and geospatial sources have been reported to show distinct trends to those obtained through pedestrian level image analysis (Long and Liu 2017; Kumakoshi et al. 2020). On the other hand, a recent publication that focused on the assessment of results obtained from varied SVI sources to address the effect of panoramic or non-panoramic views based on image distortion aspect ratios or fields of view, demonstrated that the results using distinct SVI sources showed comparable results (Biljecki et al. 2023).

This research compares 2 methodologies used to assess the view accessibility of street trees and proposes potential next steps for tree view assessment. Method 1 uses SVIs and semantic classification to define green view indicators using 360° Google Street View (GSV) images. Method 2 uses two-dimensional geospatial urban viewshed analysis. Geospatial visual corridor, viewshed, or isovist analysis approaches have been used by architects and urban planners to develop urban navigation analysis, urban escape route planning, or studies focusing on urban fabric geometry on citizen stress levels amongst others (Sander and Manson 2007; Cai et al. 2023). However, for the study of street tree view accessibility assessments, their application remains limited (Labib et al. 2021; Cimburova and Blumentrath 2022).

Using the proposed methods, this research aimed at the following objectives:

1. Compare the tree view visibility indicators and assess the variable explanation between indicators;
2. Propose SVI based indicators to assess tree view accessibility; and,
3. Identify the advantages and challenges of viewshed analysis to compute tree visibility.

A case study focusing on 2 municipalities (Saint Gilles and Molenbeek) located in the Brussels Capital Region (BCR) is presented. Using the 2 methods, tree visibility was computed and results were compared. Given that access to geospatial data remains limited in many cities while SVIs are becoming increasingly available covering large regions, the potential use of SVI indicators to explain the geospatial tree area viewshed is also assessed.

MATERIALS AND METHODS

Datasets for the Studied Municipalities

Making use of geospatial data readily available for the Brussels Capital Region, the building boundary information, street axes, and tree canopy areas were identified for the 2 municipalities under study. SVIs were also collected using 360° GSV images, and the geotagging of each image was saved and stored as a geospatial point array. In total 5,816 points (i.e., same number as the geo-tagged panoramic images) were studied for Saint Gilles, and 10,682 for Molenbeek. For more information on the data sources, see Table 1.

Method 1: Google Street View Imagery

Through queries from Street View Download 360° (Orlita 2023), all available geo-tagged 360° SVIs were compiled for both municipalities. In average, the SVIs are approximately 10 m apart from each other and located at central positions of the street canyons. Following the image compilation, a semantic classification was developed with the Python library PixelLib—implemented with Deeplabv3+ framework (Olafenwa 2021). The training datasets based on Ade20k have been utilized with architecture based on the model Xception (Zhou et al. 2019). The images were segmented into 14 categories: sky, road, building, car, tree, sidewalk, streetlight, sign, grass, bike, plant, person, path, and fence. From the segmented images and using the pixels comprising the grass, plant, and tree categories, the Green View Index (GVI) was computed (see Equation 1) as the division of all green pixels by all image pixels, for all images within each square. The obtained ratios include total UGI, Green ratio (G_r) which is the GVI, and those distinguished by types for the Tree ratio (T_r) and Grass ratio (GR_r)(Figure 1).

$$GVI = \frac{\sum_{i=1}^{n} Area_{gi}}{\sum_{i=1}^{n} Area_{ai}} \times 100 \quad (1)$$

Using the segmented images, indicators that describe the location of the UGI relative to the image boundaries were derived. These indicators include the Green Vertical angle (GV_a), the Tree Vertical angle (TV_a), and the Grass Vertical angle (GRV_a), and provide insights about the relative position and scale of the UGI. Aside from the total metrics, the Green Vertical top angle (GV_{ta}), the Tree Vertical top angle (TV_{ta}), the Grass Vertical top angle (GRV_{ta}), the Green Vertical bottom angle (GV_{ba}), the Tree Vertical bottom angle (TV_{ba}), and the Grass Vertical bottom angle (GRV_{ba}) have been computed. These angles enable capturing the relative size (e.g., crown width) and position of the UGI. The smaller the GV_{ta} and GV_{ba}, for example, the closer the UGI is to the user, and depending on the Green Horizontal angle (GH_a) and GV_a ratio, the type of UGI can be derived (see Figures 1 and 2 and Table 2).

Table 1. Data types and data sources. srf (spectral response functions).

Data type	Dataset title	Data source	Year acquisition	Method applied
Building footprint	UrbAdm_BUILDING	UrbIS	2022	M2_Viewshed
Municipality boundaries	UrbAdm_MUNICIPAL	UrbIS	2022	M1_GSV M2_Viewshed
Vegetation canopy srf 2020	vegetation_2020_canopy	Brussels Environment	2020	M2_Viewshed
Google Street View points	PointGSV	Google Street View	2009–2021	M1_GSV M2_Viewshed
Google Street View 360 images	Original file name_index of panorama_index padded _panorama id_latitude_longitude_elevation in EGM96 meters_north rotation_zoom level_year taken_month taken_day taken	Google Street View	2009–2021	M1_GSV M2_Viewshed

Table 2. Total 16 indicators. GVI (Green View Index); UGI (Urban Green Infrastructure); GSV (Google Street View).

Variable name	Description	Data
Tree View area ratio (TV_{ar})	Ratio of urban views with trees	Geospatial vector data
Green ratio (G_r)	GVI of all UGI within view	GSV imagery
Tree ratio (T_r)	GVI of trees within view	GSV imagery
Grass ratio (GR_r)	GVI of grass within view	GSV imagery
Green Vertical angle (GV_a)	Total vertical angle of UGI	GSV imagery
Green Horizontal angle (GH_a)	Total horizontal angle of UGI	GSV imagery
Green Vertical top angle (GV_{ta})	Angle from UGI to image top	GSV imagery
Green Vertical bottom angle (GV_{ba})	Angle from UGI to image bottom	GSV imagery
Tree Vertical angle (TV_a)	Total vertical angle of trees	GSV imagery
Tree Horizontal angle (TH_a)	Total horizontal angle of trees	GSV imagery
Tree Vertical top angle (TV_{ta})	Angle from trees to image top	GSV imagery
Tree Vertical bottom angle (TV_{ba})	Angle from trees to image bottom	GSV imagery
Grass Vertical angle (GRV_a)	Total vertical angle of grass patches	GSV imagery
Grass Horizontal angle (GRH_a)	Total horizontal angle of grass patches	GSV imagery
Grass Vertical top angle (GRV_{ta})	Angle grass patch to image top	GSV imagery
Grass Vertical bottom angle (GRV_{ba})	Angle grass patch to image bottom	GSV imagery

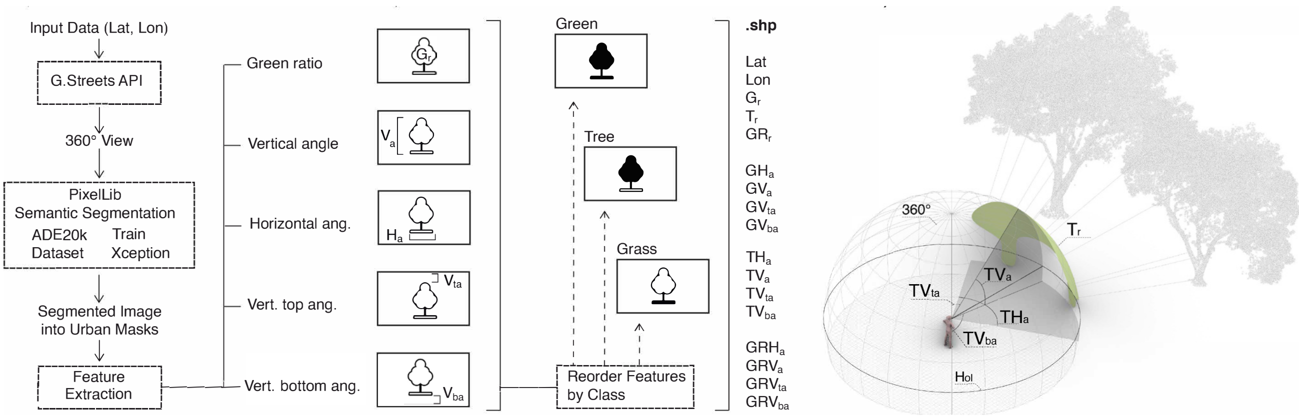

Figure 1. Left: workflow describing the GSV imagery semantic segmentation protocol and definition of indicators; Right: 3-dimensional representation of GSV tree segmentation indicators.

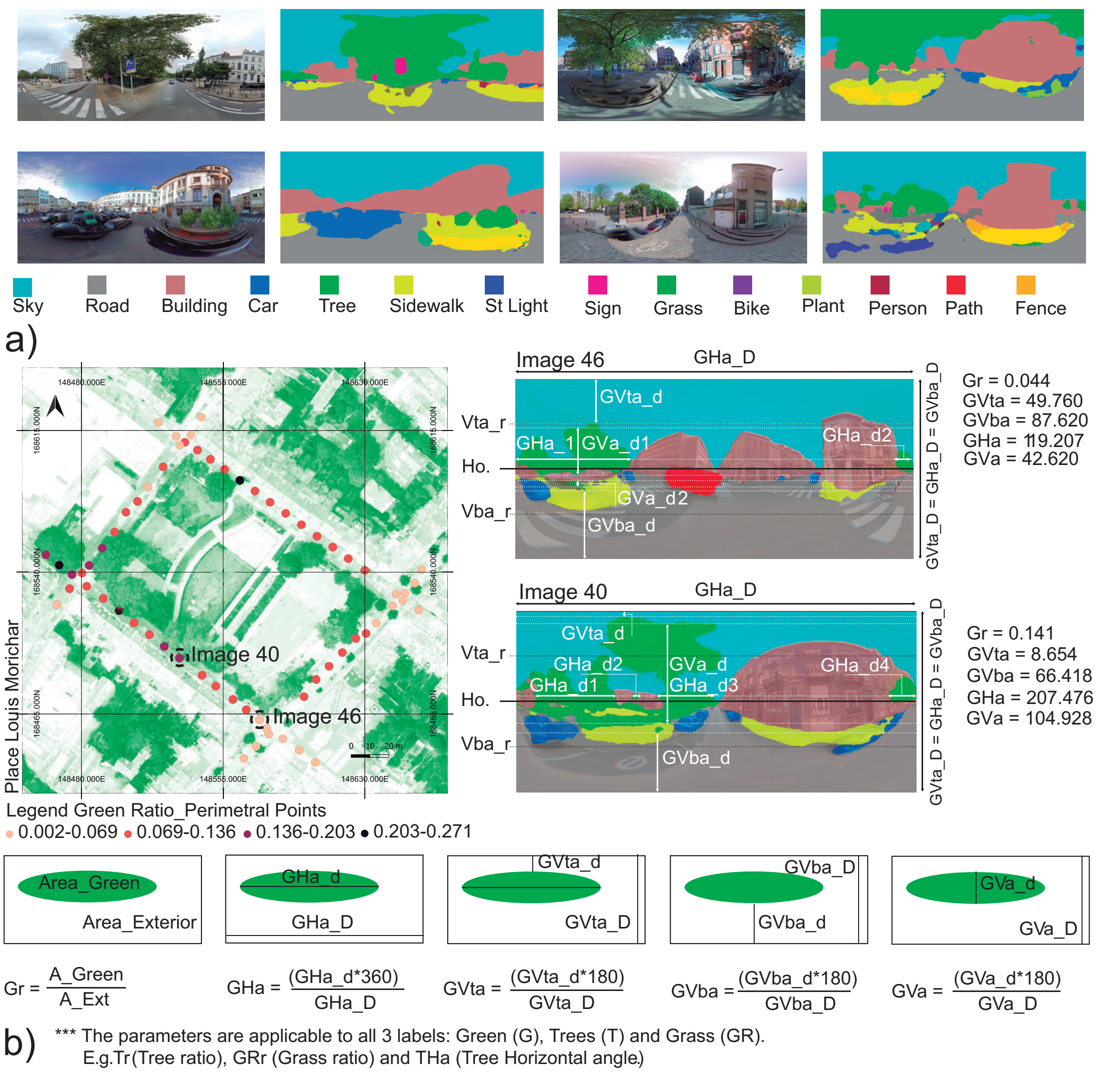

Figure 2. (a) GSV imagery segmentation classification categories color-coded; (b) green visibility indicators, displaying the results of a street surrounding a square located in Saint Gilles.

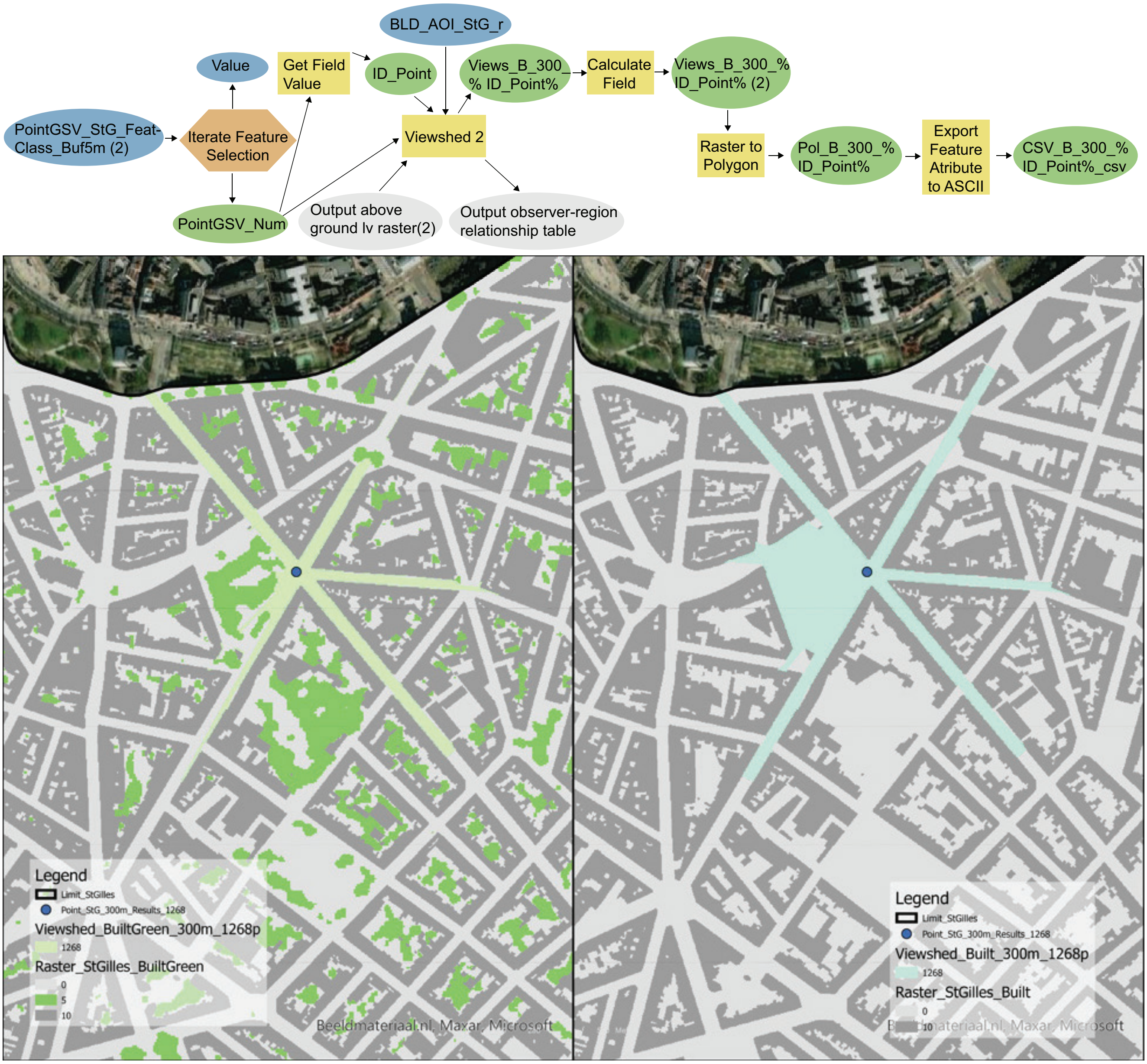

Figure 3. Viewshed analysis. Top: ModelBuilder workflow; Bottom left: including buildings and tree canopy; Bottom right: including buildings.

Method 2: Viewshed Analysis

Two-dimensional viewsheds were computed using Esri's ArcGIS Pro v2.7.3 Spatial Analyst package (Achilleos and Tsouchlaraki 2004; ArcGIS 2022) (Table 1). The tree canopy layer was made available by Brussels Environment. Details on the preparation of this dataset can be found in prior literature (van de Voorde 2017; Pelgrims et al. 2021). An iterative workflow to compute the viewshed for all points collected for Saint Gilles and Molenbeek was implemented using the ArcGIS visual programming ModelBuilder geoprocessing tool (Figure 3). The viewshed analysis was run for a spatial resolution of 1 m. Two different raster outputs were created to compute the ratio of visual area in presence of vegetation and without it from which the Tree View area ratio (TV_{ar}) was computed (Equation 2). The viewshed tool parameters are by default with a fixed outer radius of 300 m.

For the error assessment of the viewshed computation, from the 5,816 points studied for the case of

Saint Gilles, approximately 1% were run for a second and third iteration to understand if the results varied following the differences reported in prior literature (Riggs and Dean 2007; Parent and Lei-Parent 2023). For the studied TV_{ar} computations, the differences between iterations remained < 0.11% and thus it was considered negligible.

$$TVar = \frac{Area_{bg}}{Area_b} \quad (2)$$

Statistical Methods

The Pearson correlation was computed to assess the linear correlation between the studied SVI indicators and TV_{ar}. To find the group of variables that carry comparable information, the Principal Component Analysis (PCA) was studied (Pearson 1901). For dependencies that cannot be explained linearly, the random forest model as per Breiman (2001) was used to assess the nonlinear relationship between the TV_{ar} and remaining variables. The R 4.7-1.1 package for randomForest was used (Liaw and Wiener 2002). The random forest model involved randomly picking 5 variables—following the 1/3 selection of the continuous variables—from the 15 SVI indicators for each tree node which was limited to a total number of 500 trees. For validation purposes, the complete data (combing Molenbeek and Saint Gilles) was split (70% for training and 30% for testing), and the percentage of variance explained remained consistently approximately 66% on the validation sets. The assessment of the random forest model results is provided with the explained percentage of variability in TV_{ar}.

RESULTS

The summary statistics obtained from the computed 16 indicators and for both municipalities under study—Saint Gilles and Molenbeek separately—are included in Table 3. Overall, the results for Molenbeek show higher mean values (for the case of the TV_{ar}, a higher ratio indicates a lower tree area). Amongst others, the representative GV_a, TH_a, and G_r are higher for the case of Molenbeek. This is also the case for TV_{ar} obtained using the viewshed analysis.

By studying the density distribution and bar plots for all 16 indicators, the differences between the 2 municipalities become visible. For example, a higher mean TH_a and smaller TV_{ta} or TV_{ba} indicates the presence of a higher tree canopy. This is also the case for the lumped grass and tree metrics as per row 3. Similarly, for the TV_{ar} obtained following the viewshed analysis, a lower mean indicates a higher presence of trees for Molenbeek. On the other hand, overall a

Table 3. Summary statistics for all indicators and for St. Gilles (SG) and Molenbeek (M). SD (standard deviation).

Metric	SG Mean	SG SD	M Mean	M SD	Source
Tree view area ratio (TV_{ar})	0.7498	0.2653	0.5462	0.3046	Viewshed
Green ratio (G_r)	0.0286	0.0512	0.0651	0.0937	GSV
Tree ratio (T_r)	0.0269	0.0497	0.0540	0.0789	GSV
Grass ratio (GR_r)	0.0017	0.0056	0.0111	0.0289	GSV
Green Vertical angle (GV_a)	31.7790	30.9766	47.0964	36.8947	GSV
Green Horizontal angle (GH_a)	70.2803	85.3687	134.2559	118.0659	GSV
Green Vertical top angle (GV_{ta})	88.0449	60.3753	69.1991	51.2076	GSV
Green Vertical bottom angle (GV_{ba})	109.4895	45.1618	89.5474	40.6408	GSV
Tree Vertical angle (TV_a)	27.9400	27.3526	38.1327	29.8119	GSV
Tree Horizontal angle (TH_a)	64.8117	82.2655	116.8236	109.6277	GSV
Tree Vertical top angle (TV_{ta})	89.3286	61.6386	70.3443	53.1691	GSV
Tree Vertical bottom angle (TV_{ba})	115.4291	42.4438	100.7232	36.0163	GSV
Grass Vertical angle (GRV_a)	3.2670	7.7272	10.8927	16.2936	GSV
Grass Horizontal angle (GRH_a)	14.9524	37.6440	58.9782	91.2223	GSV
Grass Vertical top angle (GRV_{ta})	161.3553	34.4070	138.9791	42.5717	GSV
Grass Vertical bottom angle (GRV_{ba})	153.8602	48.1636	122.2653	60.2061	GSV

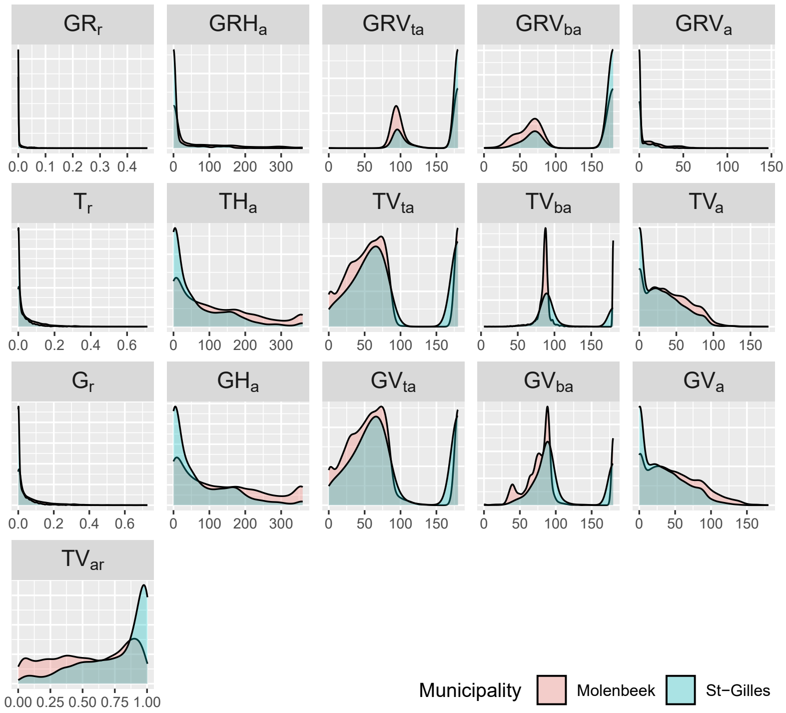

Figure 4. Density distribution plots of the studied 16 indicators. The results for Molenbeek are shown in red and in blue for Saint Gilles.

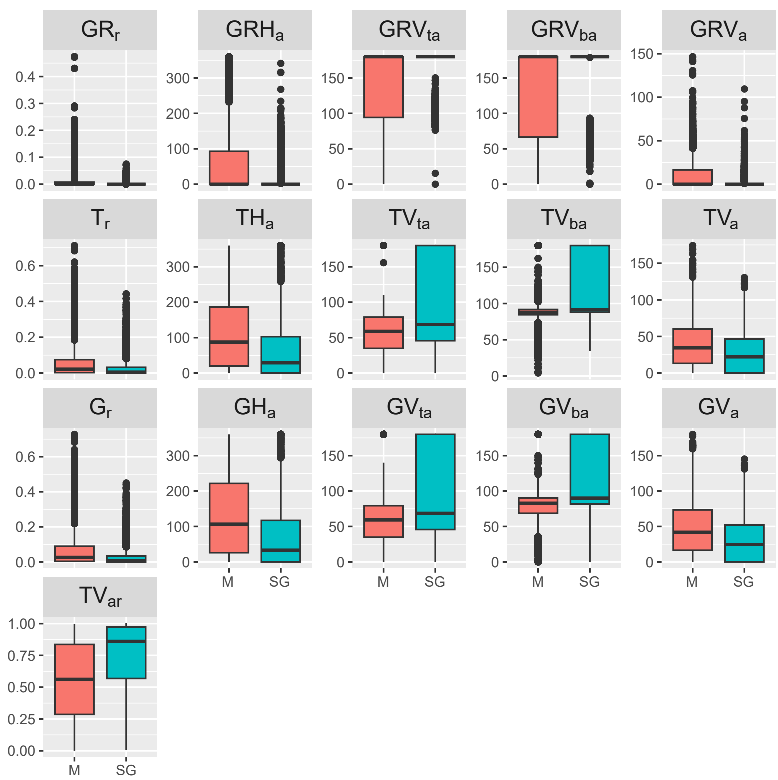

Figure 5. Box plots of the studied 16 indicators. In the left column, the results for Molenbeek (M) are shown, and in the right column, those for Saint Gilles (SG).

Figure 6. Method 2 viewshed analysis result showing the TV_{ar}. Top: Molenbeek; Bottom: Saint Gilles.

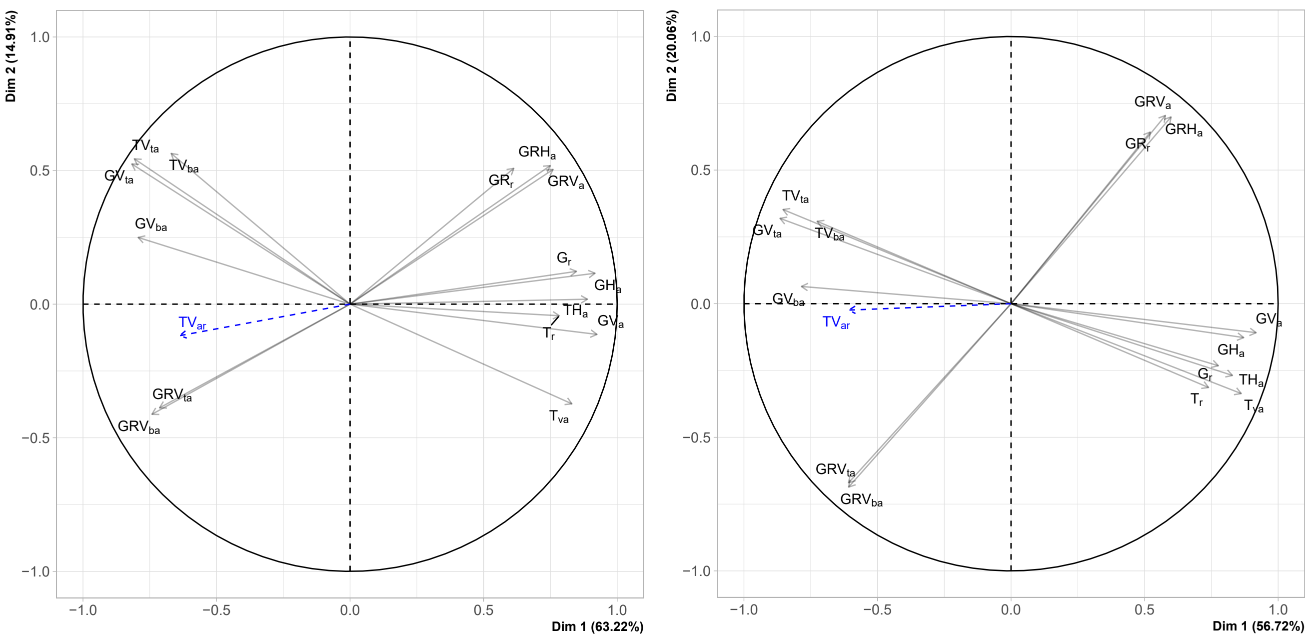

Figure 7. Principal component analysis plots for the studied indicators using the proposed methods. Left: Molenbeek; Right: Saint Gilles.

Table 4. Pearson correlation results with TV_{ar} (tree view area ratio) as the dependent variable and for Molenbeek (M) and Saint Gilles (SG). GR_R (grass ratio); GRH_A (Grass Horizontal angle); GRV_{ta} (Grass Vertical top angle); GRV_{ba} (Grass Vertical bottom angle); GRV_a (Grass Vertical angle); T_r (Tree ratio); TH_a (Tree Horizontal angle); TV_{ta} (Tree Vertical top angle); TV_{ba} (Tree Vertical bottom angle); TV_a (Tree Vertical angle); G_r (Green ratio); GH_a (Green Horizontal angle); GV_{ta} (Green Vertical top angle); GV_{ba} (Green Vertical bottom angle); GV_a (Green Vertical angle).

	GR_r	GRH_a	GRV_{ta}	GRV_{ba}	GRV_a	T_r	TH_a	TV_{ta}	TV_{ba}	TV_a	G_r	GH_a	GV_{ta}	GV_{ba}	GV_a
M	−0.41	−0.58	0.53	0.52	−0.51	−0.4	−0.64	0.46	0.39	−0.45	−0.5	−0.67	0.45	0.46	−0.54
SG	−0.38	−0.42	0.38	0.35	−0.34	−0.5	−0.57	0.49	0.34	−0.52	−0.53	−0.59	0.48	0.36	−0.54

larger variability is observed for Saint Gilles for various indicators such as TV_a or TV_{ba} which indicates a more uneven distribution of the tree canopy in this municipality. The density plots also show tree concentration peaks for the municipality of Saint Gilles, which is observable for example by studying the indicator TH_a, while for Molenbeek a more even distribution is observed. This is also the case for the TV_{ar} computed using the viewshed analysis (Figures 4 and 5). In the map visualizations of the results obtained following Method 2 viewshed analysis, it is also qualitatively visible that street tree distributions are different between the municipalities (Figure 6).

The PCA results for Saint Gilles show 4 main indicator groups: (i) the variables TV_{ta}, TV_{ba}, GV_{ta}, and GV_{ba}, which are indicators of the height of the tree; (ii) the grass related indicators GRV_a, GRH_a, or GR_r; (iii) those inversely correlated GRV_{ta} and GRV_{ba} to the vertical component, which highlight that these are independent to the tree metrics; and (iv) T_r, G_r, TH_a, or GH_a, which reflect upon the tree crown width. In the case of Molenbeek, while the 4 indicator groups are also visible, they are more dispersed, particularly those related to the crown width (i.e., T_r or TH_a), which are more differentiated from the GH_a or G_r (Figure 7). The first 2 dimensions covered approximately 75% of the variability in the data for both municipalities.

An initial study was developed to assess whether significant linear correlations were found between the studied SVI method indicators, using the viewshed TV_{ar} indicator as the dependent variable. Highest Pearson Correlation Coefficients (PCC) were observed for G_r, T_r, and TH_a with PCC approximately −0.6 ($p < 0.05$) (Table 4). However, in the data correlation, nonlinearity was observed (Figure 8), and thus, a nonlinear

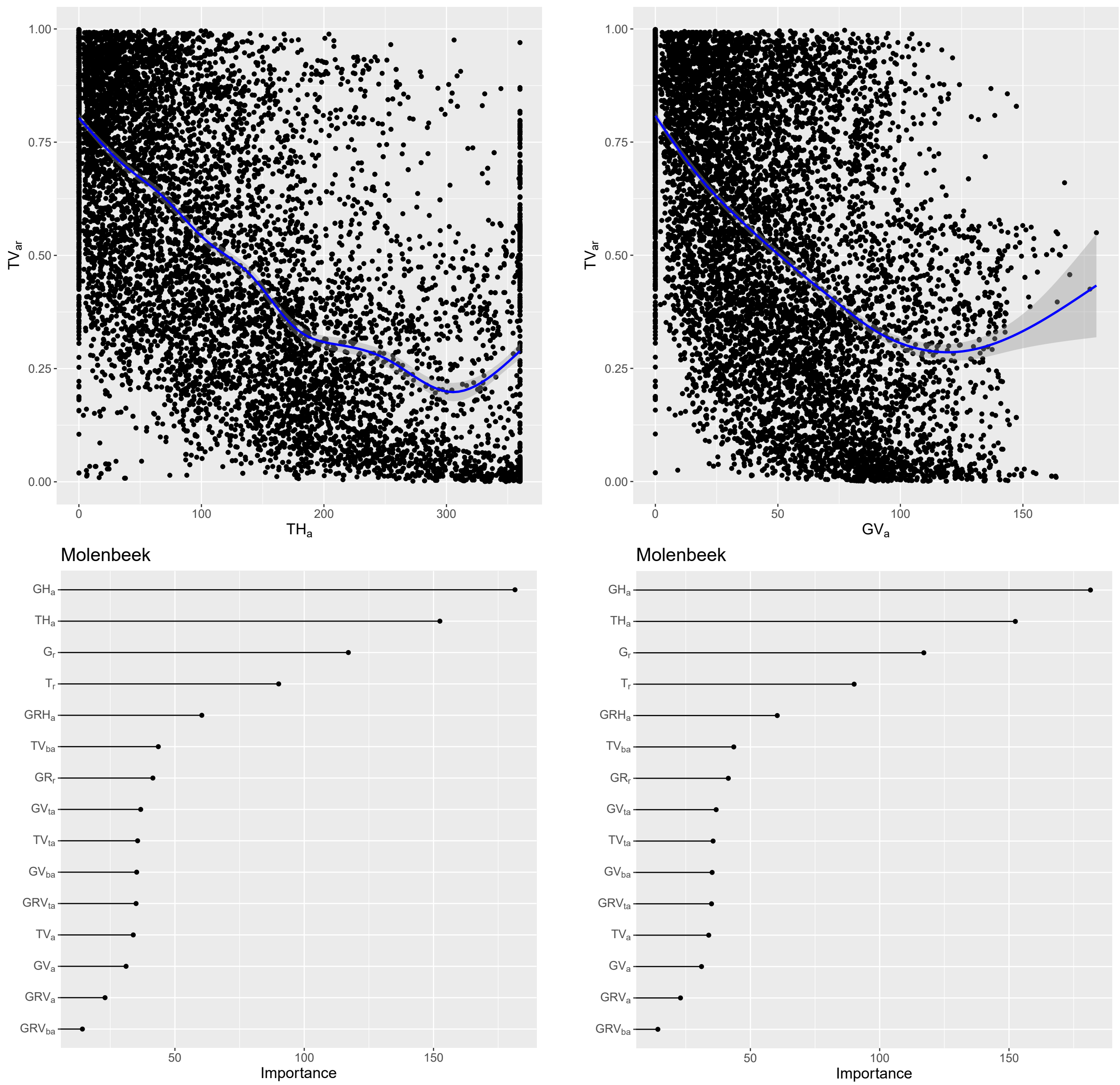

Figure 8. Top: TV_{ar} over TH_a and TV_{ar} over GV_a indicator plot and curve fit; Bottom: random forest model indicator importance ranking for both municipalities.

random forest model (Breiman 2001) was deployed, aiming to explain TV_{ar} using the indicators obtained following the SVI method. This model explained 67.32% of the variability in TV_{ar} for the case of Molenbeek, and 60.23% for the case of Saint Gilles. The 4 variables that better explained the TV_{ar} for both municipalities were the GH_a, G_r, TH_a, and T_r (Figure 8).

Limitations

The limitations identified in the proposed methodologies are to be considered. Method 1 relies on the segmentation of 360° GSV imagery which was captured between the years 2009 to 2021. Along those years, seasonal changes, natural tree growth, tree removal, or trimming may have occurred. While the GSV images are generally located at < 15 m distances, it is also possible that their geo-tagging may also include a geo-location error of approximately 2 m as reported in prior literature, as well as temporal instability which involves an incomplete date-stamp (Curtis et al. 2013; Krylov et al. 2018). Likewise, for the viewshed calculation, the tree canopy shapefile provided by Brussels Environment was used, where the Normalized Difference Vegetation Index (NDVI) was only transformed into a binary variable (presence/absence of vegetation) which may also incur potential errors (van de Voorde 2017; Pelgrims et al. 2021). Furthermore, the tree canopy database dates back to the year 2020, and thus differences with the SVIs may be found given recently planted trees or geometry changes due to tree maintenance. That is, the 30% to 40% of the unexplained variability could be related to errors derived from these limitations which could only be overcome by collecting a more accurate and up-to-date tree data documentation.

CONCLUSIONS

Focusing on all streets located at 2 municipalities from the Brussels Capital Region, the pedestrian level tree view accessibility has been studied. Two methods to compute the tree view accessibility have been compared. Using all available SVIs for the chosen municipalities and through semantic classification, the quantification of various indicators for grass, tree, and total green, as well as indicators to address their relative position within the panoramic image were proposed. Two-dimensional geospatial viewshed analysis has been deployed for the same geo-locations SVIs were available for, and the Tree View area ratio (TV_{ar}) was computed. To assess whether the SVI green view indicators can explain the viewshed analysis results, an initial linear correlation was studied using TV_{ar} as the dependent variable. Significant correlations were observed particularly between the indicators related with the tree crown width such as TH_a or GH_a, with PCC approximately −0.6 (note that a low ratio of TV_{ar} denotes a larger tree view area). Nonlinearity was observed in the data, thus subsequently, a random forest model was deployed which explained approximately 70% variability of the TV_{ar} for Molenbeek and approximately 60% for Saint Gilles. The remaining unexplained 30% to 40% variability could also be attributable to the limitations of the utilized datasets such as geo-location errors or date incongruencies, as well as to errors due to the remote sensing data processing, which can affect the accuracy of the geospatial tree canopy layer.

Overall, SVI tree view indicators provide acceptable predictions of the pedestrian level tree canopy viewshed, which could be particularly useful for municipalities with no access to detailed geospatial data. In all cases, the computational costs associated with the tree view access analysis won't be negligible, thus the challenges for their implementation for urban planning practices are yet to be overcome.

Future work will involve a three-dimensional characterization of the tree canopy, using detailed digital elevation models and urban point clouds which are starting to be collected by several municipalities. Working with three-dimensional meshes can enable the computation of the viewshed analysis around a tree from various angles and better describe the tree trunk and crown geometries.

LITERATURE CITED

Achilleos G, Tsouchlaraki A. 2004. Visibility and viewshed algorithms in an information system for environmental management. In: Brebbia CA, editor. *Management Information Systems 2004: Incorporating GIS and Remote Sensing*. WIT Transactions on Information and Communication Technologies. Southampton (United Kingdom): WIT Press. p. 109-121. https://doi.org/10.2495/MIS040121

ArcGIS. 2022. *Geodesic viewshed. ArcGIS Pro 2.7 documentation*. https://pro.arcgis.com/en/pro-app/2.7/tool-reference/3d-analyst/viewshed-2.htm

Biljecki F, Zhao T, Liang X, Hou Y. 2023. Sensitivity of measuring the urban form and greenery using street-level imagery: A comparative study of approaches and visual perspectives. *International Journal of Applied Earth Observation and Geoinformation*. 122:103385. https://doi.org/10.1016/j.jag.2023.103385

Breiman L. 2001. Random forests. *Machine Learning*. 45(1):5-32. https://doi.org/10.1023/A:1010933404324

Cai M, Xiang L, Ng E. 2023. How does the visual environment influence pedestrian physiological stress? Evidence from high-density cities using ambulatory technology and spatial machine learning. *Sustainable Cities and Society*. 96:104695. https://doi.org/10.1016/j.scs.2023.104695

Cimburova Z, Blumentrath S. 2022. Viewshed-based modelling of visual exposure to urban greenery—An efficient GIS tool for practical planning applications. *Landscape and Urban Planning*. 222:104395. https://doi.org/10.1016/j.landurbplan.2022.104395

Curtis JW, Curtis A, Mapes J, Szell AB, Cinderich A. 2013. Using google street view for systematic observation of the built environment: Analysis of spatio-temporal instability of imagery dates. *International Journal of Health Geographics*. 12(1):53. https://doi.org/10.1186/1476-072X-12-53

de Vries S, van Dillen SME, Groenewegen PP, Spreeuwenberg P. 2013. Streetscape greenery and health: Stress, social cohesion and physical activity as mediators. *Social Science & Medicine*. 94:26-33. https://doi.org/10.1016/j.socscimed.2013.06.030

Frederiksberg Kommune. 2018. *Frederiksberg Kommunes Traepolitik*. Frederiksberg (Denmark): Frederiksberg Kommune. https://www.frederiksberg.dk/media/znzn1xq2/traepolitik.pdf

Hartig T. 2008. Green space, psychological restoration, and health inequality. *The Lancet*. 372(9650):1614-1615. https://doi.org/10.1016/S0140-6736(08)61669-4

Hartig T, Kahn PH. 2016. Living in cities, naturally. *Science*. 352(6288):938-940. https://doi.org/10.1126/science.aaf3759

Hu Y, Wang H, Yan H, Han Q, Nan X, Zhao K, Bao Z. 2023. Alternative scenarios for urban tree surveys: Investigating the species, structures, and diversities of street trees using street view imagery. *Science of The Total Environment*. 895:165157. https://doi.org/10.1016/j.scitotenv.2023.165157

Huang S, Qi J, Li W, Dong J, van den Bosch CK. 2021. The contribution to stress recovery and attention restoration potential of exposure to urban green spaces in low-density residential areas. *International Journal of Environmental Research and Public Health*. 18(16):8713. https://doi.org/10.3390/ijerph18168713

Konijnendijk CC. 2023. Evidence-based guidelines for greener, healthier, more resilient neighbourhoods: Introducing the 3–30–300 rule. *Journal of Forestry Research*. 34(3):821-830. https://doi.org/10.1007/s11676-022-01523-z

Krylov V, Kenny E, Dahyot R. 2018. Automatic discovery and geotagging of objects from street view imagery. *Remote Sensing*. 10(5):661. https://doi.org/10.3390/rs10050661

Kumakoshi Y, Chan SY, Koizumi H, Li X, Yoshimura Y. 2020. Standardized green view index and quantification of different metrics of urban green vegetation. *Sustainability*. 12(18):7434. https://doi.org/10.3390/su12187434

Labib SM, Huck JJ, Lindley S. 2021. Modelling and mapping eye-level greenness visibility exposure using multi-source data at high spatial resolutions. *Science of The Total Environment*. 755:143050. https://doi.org/10.1016/j.scitotenv.2020.143050

Li X, Zhang C, Li W, Ricard R, Meng Q, Zhang W. 2015. Assessing street-level urban greenery using Google Street View and a modified green view index. *Urban Forestry & Urban Greening*. 14(3):675-685. https://doi.org/10.1016/j.ufug.2015.06.006

Liaw A, Wiener M. 2002. Classification and regression by randomForest. *R News*. 2(3):18-22. https://cran.r-project.org/doc/Rnews/Rnews_2002-3.pdf

Long Y, Liu L. 2017. How green are the streets? An analysis for central areas of Chinese cities using Tencent Street View. *PLOS ONE*. 12(2):e0171110. https://doi.org/10.1371/journal.pone.0171110

Masterson V. 2022. The best way to keep cool in heatwaves? Plant 170,000 trees, according to Paris. Cologny (Switzerland): World Economic Forum. https://www.weforum.org/agenda/2022/08/paris-trees-climate-change

Million Trees NYC. 2017. *Million Trees NYC*. https://www.milliontreesnyc.org

Olafenwa A. 2021. *Simplifying object segmentation with PixelLib library*. https://vixra.org/pdf/2101.0122v1.pdf

Orlita T. 2023. *Google Street View Download 360*. [Accessed 2022 September 28]. https://svd360.istreetview.com

Parent JR, Lei-Parent Q. 2023. Rapid viewshed analyses: A case study with visibilities limited by trees and buildings. *Applied Geography*. 154:102942. https://doi.org/10.1016/j.apgeog.2023.102942

Pearson K. 1901. LIII. On lines and planes of closest fit to systems of points in space. *The London, Edinburgh, and Dublin Philosophical Magazine and Journal of Science*. 2(11):559-572. https://doi.org/10.1080/14786440109462720

Pelgrims I, Devleesschauwer B, Guyot M, Keune H, Nawrot TS, Remmen R, Saenen ND, Trabelsi S, Thomas I, Aerts R, de Clercq EM. 2021. Association between urban environment and mental health in Brussels, Belgium. *BMC Public Health*. 21(1):635. https://doi.org/10.1186/s12889-021-10557-7

Riggs PD, Dean DJ. 2007. An investigation into the causes of errors and inconsistencies in predicted viewsheds. *Transactions in GIS*. 11(2):175-196. https://doi.org/10.1111/j.1467-9671.2007.01040.x

Sander HA, Manson SM. 2007. Heights and locations of artificial structures in viewshed calculation: How close is close enough? *Landscape and Urban Planning*. 82(4):257-270. https://doi.org/10.1016/j.landurbplan.2007.03.002

Tabatabaie S, Litt JS, Muller BHF. 2023. Sidewalks, trees and shade matter: A visual landscape assessment approach to understanding people's preferences for walking. *Urban Forestry & Urban Greening*. 84:127931. https://doi.org/10.1016/j.ufug.2023.127931

Triebner K, Markevych I, Hustad S, Benediktsdóttir B, Forsberg B, Franklin KA, Gullón Blanco JA, Holm M, Jaquemin B, Jarvis D, Jõgi R, Leynaert B, Lindberg E, Martínez-Moratalla J, Muniozguren Agirre N, Pin I, Sánchez-Ramos JL, Heinrich J, Gómez Real F, Dadvand P. 2019. Residential surrounding greenspace and age at menopause: A 20-year European study (ECRHS). *Environment International*. 132:105088. https://doi.org/10.1016/j.envint.2019.105088

van de Voorde T. 2017. Spatially explicit urban green indicators for characterizing vegetation cover and public green space proximity: A case study on Brussels, Belgium. *International Journal of Digital Earth*. 10(8):798-813. https://doi.org/10.1080/17538947.2016.1252434

van den Bosch M, Ode Sang Å. 2017. Urban natural environments as nature-based solutions for improved public health—A systematic review of reviews. *Environmental Research*. 158:373-384. https://doi.org/10.1016/j.envres.2017.05.040

Ville de Liege. 2007. *Plan Canopee*. https://www.yumpu.com/fr/document/view/65987939/plan-canopee-ville-de-liege

Ye Y, Richards D, Lu Y, Song X, Zhuang Y, Zeng W, Zhong T. 2019. Measuring daily accessed street greenery: A human-scale approach for informing better urban planning practices. *Landscape and Urban Planning*. 191:103434. https://doi.org/10.1016/j.landurbplan.2018.08.028

Zhou B, Zhao H, Puig X, Xiao T, Fidler S, Barriuso A, Torralba A. 2019. Semantic understanding of scenes through the ADE20K dataset. *International Journal of Computer Vision*. 127(3):302-321. https://doi.org/10.1007/s11263-018-1140-0

ACKNOWLEDGEMENTS

This research was funded by the Louvain4City 2021 Grant from UCLouvain.

M. Llaguno-Munitxa (corresponding author)
Université Catholique de Louvain, LOCI-LAB
Pl. du Levant 1
Ottignies-Louvain-la-Neuve, Belgium
maider.llaguno@uclouvain.be

E. Agudo-Sierra
Université Catholique de Louvain, LOCI-LAB
Pl. du Levant 1
Ottignies-Louvain-la-Neuve, Belgium

A. Burgueño-Diaz
Calle de los Hermanos García Noblejas
Madrid, Spain

Alain Guillet
Louvain Institute of Data Analytics and Modeling
Economics and Statistics
Ottignies-Louvain-la-Neuve, Belgium

Conflicts of Interest:
The authors reported no conflicts of interest.